

Scientific paper

Inhibition of Copper Corrosion Studied by Electrochemical and EQCN Techniques

Matjaž Finšgar^a, Ingrid Milošev*^a and Boris Pihlar^b^a Jožef Stefan Institute, Department of Physical and Organic Chemistry, Jamova 39, SI-1000 Ljubljana, Slovenia^b Faculty of Chemistry and Chemical Technology, University of Ljubljana, Aškerčeva 5, SI-1000 Ljubljana, Slovenia.

* Corresponding author: E-mail: ingrid.milosev@ijs.si

Received: 20-12-2006

Abstract

The inhibition of copper corrosion in 3% NaCl solution in the absence and presence of an organic inhibitor was studied by using different electrochemical techniques, i.e. cyclic voltammetry, linear polarization, Tafel plots and potentiodynamic curves on bulk Cu electrode. Two organic inhibitors were investigated (3-amino-1,2,4-triazole – ATA and benzotriazole – BTAH). Experimental results show that BTAH is a more effective inhibitor than ATA.

Electrochemical quartz crystal nanobalance (EQCN) was applied to deposit copper on a gold electrode by using controlled potential or controlled current deposition method. It was found that deposition of copper was better using controlled potential technique. The process of film formation on copper plated on gold was studied in 3 % sodium chloride in the absence and presence of ATA or BTAH. Selected corrosion inhibitors showed very rapid interaction between the metal surface and organic molecules. Results have shown that *in-situ* EQCN is a powerful technique for obtaining information on corrosion inhibition and its mechanism.

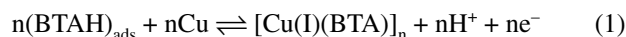
Keywords: Copper, chlorides, EQCN, benzotriazole, 3-amino-1,2,4-triazole

1. Introduction

Copper is used in different fields of industry, especially in electronics. Because of relatively good corrosion resistance it is used in constructions of waterworks networks. However, in a medium which contains chloride, sulphate and nitrate ions copper easily corrodes. Therefore, the protection of copper surface saves large costs on repairs and equipment replacements. It is known that heterocyclic organic molecules which can donate electron pair are potential corrosion inhibitors. Due to interaction of an inhibitor and a metal, the metal surface is modified and the metal surface is protected. Potential inhibitors which are effective in neutral and basic solutions are azoles, triazoles and sulfoxides.^{1,2,3} Due to their ability of bonding to transition metals organic compounds that contain nitrogen or sulfur atoms are effective inhibitors to corrosion of copper.

One of the most effective inhibitors for copper is 1-H-benzotriazole (BTAH). Cotton⁴ showed that BTAH in a neutral medium in the presence of Cu⁺ and Cu²⁺ ions, forms yellow and green precipitates. It was assumed that copper ions bond via triazole ring. Recent studies have shown that there are two mechanisms of bonding BTAH

to the copper surface. The first mechanism predicts the adsorption of BTAH on the copper surface.⁵ The second mechanism predicts the formation of polymeric complexes with Cu(I) ions (Cu⁺BTA⁻).⁵ BTAH molecules adsorb on copper from solutions with a low pH, at the negative electrode potential and low concentration of the inhibitor, meanwhile the formation of polymeric complexes is favorable in solutions with a higher pH, at the positive electrode potential and higher inhibitor concentration.⁶ Thus, the formation of complexes and adsorption must be somehow connected. Youda et al.⁷ have suggested equilibrium between these two processes:



Research of processes on the electrode surface requires sophisticated techniques which enable acquisition of information about the structure and composition of surface layers. Electrochemical quartz crystal microbalance (EQCM) is one of the newest techniques which are used in the field of electrochemical research of surface layers and mechanisms of corrosion inhibition. EQCM

allows simultaneous measurements of electrochemical parameters and mass change on the electrode. The core of EQCM is a quartz crystal, which is sandwiched between two electrodes. The first one of two electrodes (the outer electrode) is exposed to the observed medium, and the second one is inside the crystal holder. Frequently, the electrodes are made of platinum or gold. The purpose of these two electrodes is to induce an electric field which causes mechanic oscillation of quartz crystal (piezoelectric effect). A small mass change on outer electrode causes an interruption of resonance frequency. According to Sauerbrey equation, frequency alteration Δf is related to mass change Δm :

$$\Delta f = -\frac{2\Delta m f_0^2 n}{A\sqrt{\mu\rho}}, \quad (2)$$

where f_0 is the resonant frequency of the quartz oscillator, n is the overtone number, A is the surface area, ρ is the quartz density (2.65 g cm^{-3}), and μ is the shear modulus of quartz ($2.95 \cdot 10^{11} \text{ g cm}^{-1} \text{ s}^{-2}$). Equation 2 shows that when the mass on electrode increases, the resonant frequency decreases. In this way, it is possible to detect a mass change of 1 ng cm^{-2} (therefore, we are using the term EQCN instead of EQCM, QCN – quartz crystal nanobalance). EQCN is a useful technique for studying adsorption processes, especially in the field of corrosion inhibition, because of the high sensitivity of mass change.⁸

The purpose of this work was to study the interaction between benzotriazole and 3-amino-1,2,4-triazole (ATA) with copper in 3% aqueous NaCl solution with different electrochemical methods and the EQCN technique.

2. Experimental

The bulk electrode used for electrochemical experiments was pure copper (99.9%) cut out from copper foil (Goodfellow, Cambridge) in the shape of disc 15 mm in diameter. Prior to each experiment the electrode was mechanically polished with SiC paper up to 4000 grid and rinsed with distilled water. BTAH was supplied by Merck (p.s. quality) and ATA by Sigma-Aldrich (purity 95%).

The specimens were embedded in Teflon holder (PAR), so that the area exposed to the solution measured 0.95 cm^2 . A saturated calomel electrode (SCE, $E = 0.2415 \text{ V vs. SHE}$) served as a reference electrode and a carbon rod as a counter electrode. All potentials in this work were measured with respect to the SCE. Experiments were carried out in a home-made three electrode corrosion cell (volume 0.35 L). Measurements were performed in 3% (w) aqueous NaCl solution in the absence and presence of 0.1, 5 and 30 mM ATA or BTAH. Cyclic voltammetry (CV) experiments, linear polarization, Tafel and potentiodynamic plots were carried out using Autolab potentiostat/galvanost model PGSTAT 12, controlled by a GPES pro-

gram. These experiments were executed in sequence after specimen being stabilized in solution for 1 h at the open circuit potential (OCP). Linear polarization and Tafel plot measurements were performed in potential range $\pm 10 \text{ mV}$ and $\pm 250 \text{ mV}$, respectively, against corrosion potential (E_{corr}) in anodic direction using 0.1 mV/s potential scan rate. Polarization resistance (R_p) and corrosion potential were determined from the attained results of linear polarization measurements with the assistance of the GPES program. Corrosion current density (j_{corr}) was determined from Tafel plots. Anodic polarization curves measurements started 250 mV more negative with respect to E_{corr} , and progressed in the anodic direction with a potential scan rate of 1 mV/s . CV measurements were performed by cycling between initial potential (-0.8 V) and different vertex potential (E_a) with 10 mV/s potential scan rate.

For EQCN experiments two gold electrodes were deposited to the adhesive layer of chromium oxide on the quartz crystal. AT-cut quartz crystal had 5 MHz nominal frequency. The crystal was installed in TPS 550 Teflon holder (Maxtek) connected to Maxtek PM-710 EQCN instrument. Outer electrode located at the solid-liquid interface had an area of 1.37 cm^2 . Copper was electroplated on gold electrode from 0.5 M CuSO_4 , $1 \text{ M C}_2\text{H}_5\text{OH}$ and $1 \text{ M H}_2\text{SO}_4$ solution: a) potentiostatically, with controlled working electrode potential and b) galvanostatically, with controlled current.

X-ray diffraction measurements were performed on D4 Endeavor spectrometer (Bruker AXD). The specimen surface was photographed using an Olympus BX5I optical microscope.

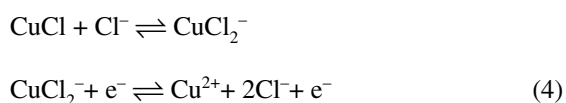
3. Results and Discussion

3.1. Electrochemical Measurements at the Bulk Cu Electrode

Figure 1 shows electrochemical behavior of copper in 3% NaCl solution in the range from -0.8 V to 0.6 V . The cyclic voltammogram shows two anodic peaks at 0.12 V and 0.29 V , respectively, and only one cathodic peak at -0.23 V . The anodic peak A_1 at 0.12 V corresponds to the formation of CuCl layer:^{9,10}



This film is porous and it allows the reaction to continue by diffusion of Cl^- through the pores of CuCl. The second anodic peak (labeled A_2) appears at more positive potential, which is due to the formation of Cu^{2+} ions according to the following equations:¹¹



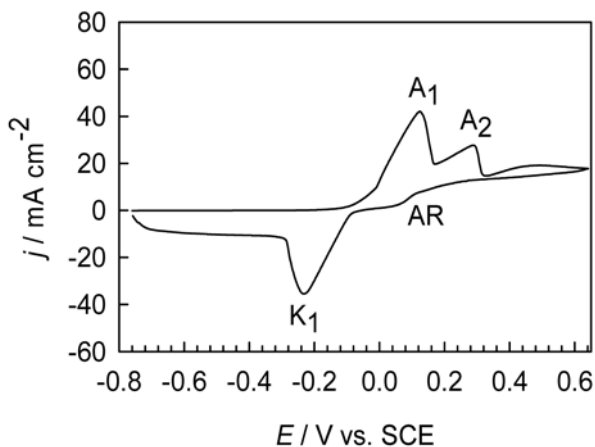


Figure 1: Cyclic voltammograms of Cu in 3% NaCl solution, $\nu = 10 \text{ mV s}^{-1}$.

Following the peak A_2 a current plateau is established. It is ascribed to the equilibrium between dissolution of CuCl_2^- and the formation of CuCl .¹²

In cathodic cycle, at the potential of about 0.1 V, a small anodic reactivation peak was noticed (labeled AR). The appearance of an anodic peak in cathodic cycle is un-

sual. It is presumably related to the formation of poorly protective film during the anodic scan, or patches of uncorroded copper, which further corrode after the potential reversal. At more negative cathodic potentials only one cathodic peak, K_1 , appears at -0.23 V , which most likely represents the reduction of the CuCl_2^- to Cu. Otmačić et al. showed that cuprous chlorides accumulate on electrode.⁹

Figure 2 shows that in the presence of 0.1 mM ATA, both anodic (A_1 and A_2) and cathodic (K_1) peak are observed. An additional anodic peak A^* at 0.34 V is also noticed. It is supposed that this peak indicate the Cu(II)-ATA complex formation. In the presence of higher concentration of ATA (5 and 30 mM) neither of anodic peaks is clearly expressed and the peak A^* , which was noticed earlier, is transformed to the anodic plateau. In the presence of 0.1 mM BTAH the shape of curve is similar to that shown in Fig. 1 and three peaks A_1 , A_2 and K_1 are noticed. However, at higher concentrations of BTAH (5 and 30 mM), the anodic peak A_1 diminished, while anodic peak A_2 is transformed to the anodic plateau. A current hysteresis appears in the presence of 5 and 30 mM BTAH indicating its catalytic origin by triggering further dissolution of copper in cathodic direction. In solutions containing 0.1, 5 and 30

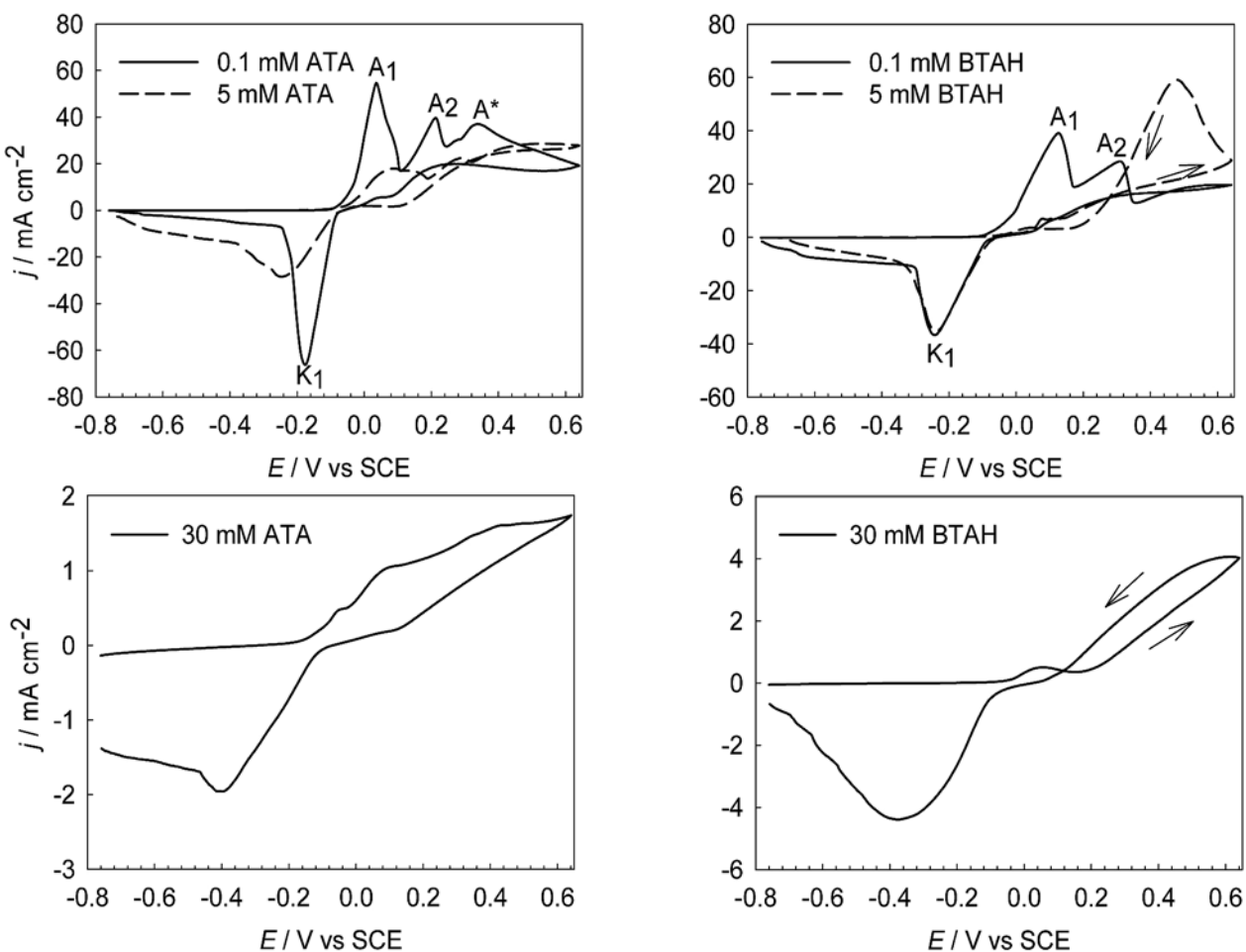


Figure 2: Cyclic voltammograms of Cu in 3% NaCl solution containing various concentrations of ATA and BTAH, $\nu = 10 \text{ mV s}^{-1}$.

mM BTAH, 5 and 30 mM ATA the current density of both anodic and cathodic peaks is significantly reduced. The current reduction can be attributed to the formation of protective film which prevents copper dissolution.

In the solution containing the lowest concentration of BTAH, 0.1 mM, the reduction in current density is observed (Fig. 2). For 0.1 mM ATA, however, the anodic and cathodic peaks increase compared to inhibitor-free solution (Fig. 1). Increase in current density is characteristic for substances with complexation properties,¹³ therefore we can assume that at low concentrations the complexation of ATA with metal ions dominates over the formation of surface layer with protective properties. The comparison of voltammograms for ATA and BTAH in Fig. 2 shows that the mechanism of their inhibition are different and that peak current densities are lower in the presence of BTAH in contrast with ATA. This shows that BTAH is a more effective inhibitor than ATA.

The total charge in anodic and cathodic direction of CV process was determined by integration of anodic and cathodic peaks. The ratio between total cathodic Q_c and total anodic Q_a charge is presented in Table 1. The film formed in anodic cycle starts to dissolve when Q_a exceeds Q_c and ratio Q_c/Q_a falls below one. Therefore, the Q_c/Q_a ratio can be taken as an indication of the formation of dissolved products. Table 1 shows that by increasing inhibitor concentration better copper surface protection is achieved. The ratio Q_c/Q_a falls below one at $E_a \geq 0.2$ V for 0.1 mM, at $E_a \geq 0.1$ V for 5 mM and at $E_a \geq 0.3$ V for 30 mM of ATA, and at $E_a \geq 0$ V for 0.1 mM, at $E_a \geq 0$ V for 5 mM and at $E_a \geq 0.3$ V for 30 mM of BTAH. The highest protection of copper surface is achieved at 30 mM BTAH. Q_a exceeds Q_c at E_a , which corresponds to the formation of CuCl_2^- (Fig. 1), so we can conclude that this is the major corrosion product in chloride solution.

During the cyclic voltammetry measurements up to high positive potentials in solution containing 5 and 30 mM BTAH, the greenish precipitate was formed. This precipitate was filtered and then dissolved in petrol ether. The crystallization was performed with the addition of distilled water. Formed crystals were examined by the X-ray diffraction, which did not give a pattern, suggesting

that the structure was amorphous or that particles were smaller than 10 nm.¹⁴

3. 2. EQCN Measurements on the Cu-plated Au Crystals

The aim of this work was to investigate which deposition method gives the best copper film on gold electrode for subsequent EQCN experiments without local defects. The quality of the deposited copper was checked under the optical microscope. The deposition of copper on gold electrode can be performed at the constant applied potential, at the constant working electrode potential (potentiostatic mode) and at the constant current electrolysis (galvanostatic mode). In potentiostatic mode three potentials were tested, -0.9 V, -0.6 V and -0.3 V, whereas in galvanostatic mode two cathodic currents were applied (6 mA and 20 mA). Examples of the deposits thus obtained are presented in Fig. 3. Under the experimental conditions of potentiostatic deposition method at -0.6 V the copper film with the smallest number of defects was obtained. On the contrary, galvanostatic deposition produced a Cu film with numerous defects and inhomogeneous surface. Thus, all further experiments started with Cu layer formed by potentiostatic deposition at -0.6 V. New Cu layer is deposited prior each experiment.

EQCN measurements of the inhibitor adsorption and the formation of protective layer on copper surface were performed on freshly deposited copper layer. The adsorption processes were carried out in 3% NaCl solution in the presence of 30 mM ATA or BTAH. The one-hour exposure of copper electrode to the solution containing inhibitor leads to an increase in the mass on the electrode. Two measurements for each inhibitor, ATA and BTAH, are presented in Figure 4. The inhibitors were adsorbed on copper surface as evident from an isotherm shaped mass increase with time. The adsorption is probably kinetically controlled process, since two measurements gave quite different mass changes: 26.8 and 51.1 $\mu\text{g cm}^{-2}$ for ATA, and 30.8 and 52.8 $\mu\text{g cm}^{-2}$ for BTAH. Variations in the inhibitor adsorption can be partially caused by variations of the layer characteristics. Although time and

Table 1: Ratio Q_c/Q_a for total anodic (Q_a) and total cathodic (Q_c) charge as a function of anodic potential limit (E_a) in cyclic voltammogram for Cu in 3% NaCl.

E_a [V]	NaCl	ATA (mM)			BTAH (mM)		
		0.1	5	30	0.1	5	30
-0.2	5.92	3041	38.0	128	24.3	17.0	25.4
-0.1	1.05	61.1	4.08	15.8	1.11	4.30	10.1
0	0.79	17.4	1.12	5.90	0.79	0.95	3.59
0.1	0.83	3.32	0.90	3.67	0.81	0.93	1.93
0.2	0.64	0.95	0.71	1.48	0.60	0.90	1.19
0.3	0.52	0.79	0.46	0.98	0.47	0.59	0.78
0.4	0.46	0.78	0.36	0.82	0.40	0.32	0.75
0.5	0.42	0.73	0.32	0.73	0.38	0.23	0.75
0.6	0.40	0.68	0.36	0.63	0.36	0.27	0.75

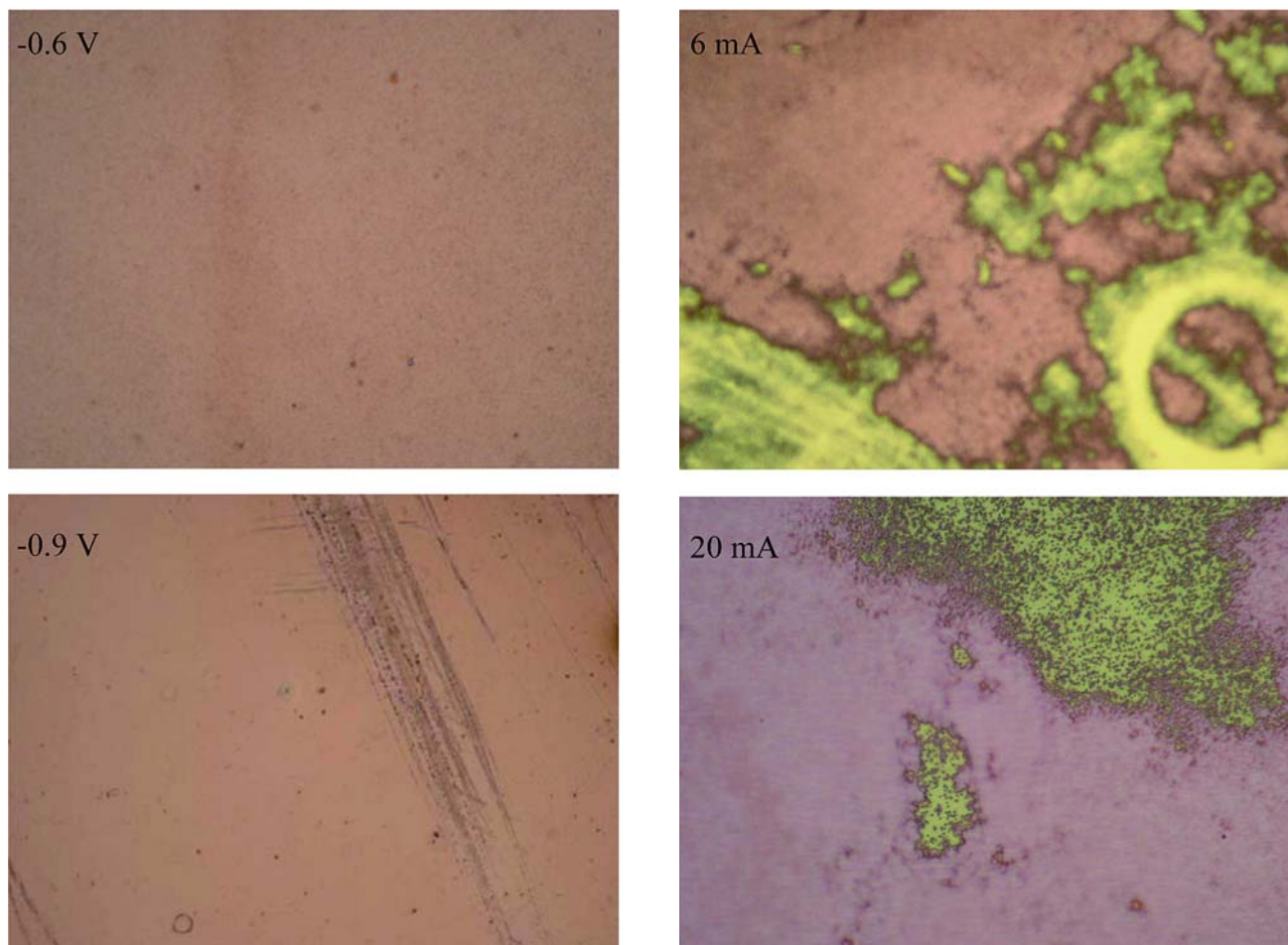


Figure 3: Microscopic image of deposited copper by the potentiostatic (left) and galvanostatic (right) mode (magnification 100 X).

potential of adsorption were constant, possible variations in homogeneity, surface and morphological properties may affect the inhibitor adsorption. Both adsorption processes show that after 3 minutes immersion the curve

changes its slope (denoted by arrow). We assume that the adsorption may include several adsorption steps and/or a reorientation may appear at this coverage due to the mutual interactions between adsorbed molecules.

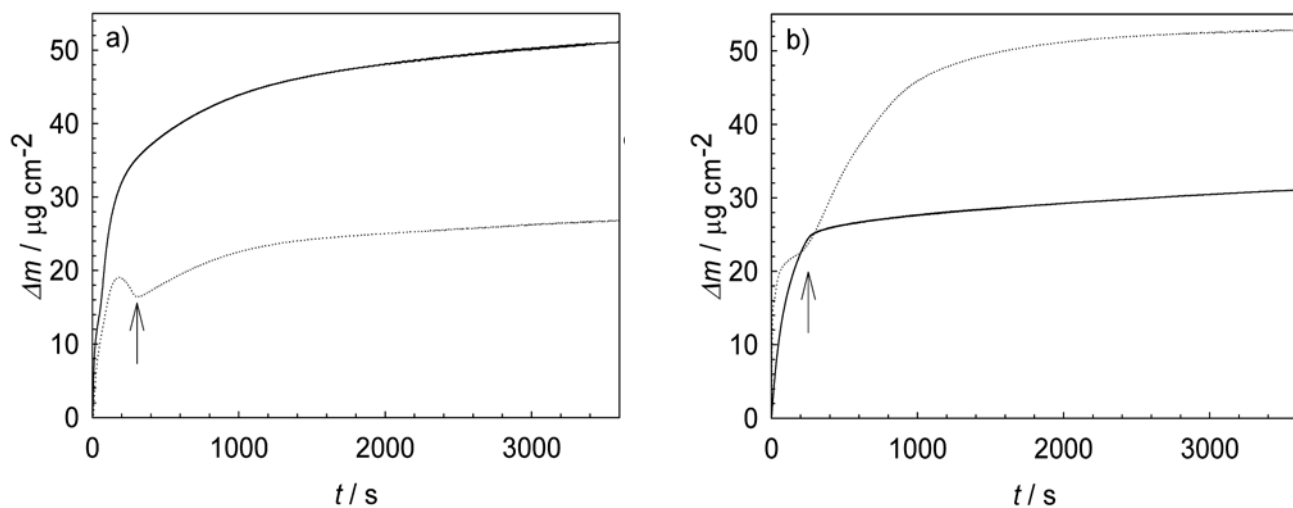


Figure 4: The change in mass measured on Cu-plated electrode during exposure in 3% NaCl containing (a) 30 mM ATA and (b) 30 mM BTAH. Two measurements for each inhibitor are presented; new Cu layer is deposited prior each measurement.

After a one-hour exposure of the Cu-plated electrode to the solution containing 30 mM ATA or BTAH (Δm for ATA was $51.1 \mu\text{g cm}^{-2}$ and for BTAH $52.8 \mu\text{g cm}^{-2}$), the electrodes were transferred into pure 3% NaCl solution and the protective properties of the formed film were followed. Figure 5 clearly shows that the surface layer formed in the presence of inhibitor BTAH protects copper surface very well and for longer time periods, while that formed in the presence of the inhibitor ATA dissolves readily. The mass change after 6000 s exposure was $-0.045 \mu\text{g cm}^{-2}$ for BTAH and $-99.6 \mu\text{g cm}^{-2}$ for ATA.

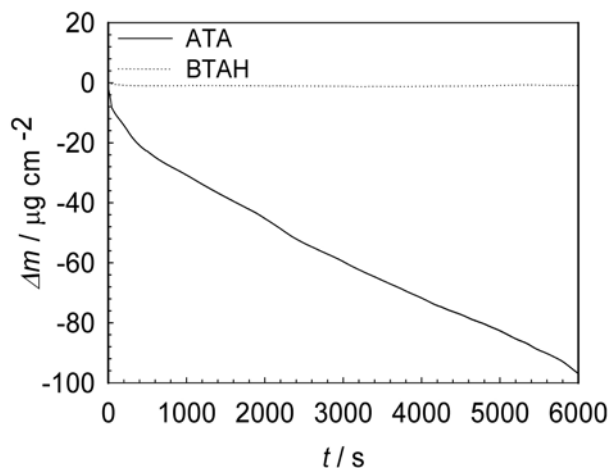


Figure 5: The change in mass of the surface layer on Cu-plated electrode in 3% NaCl solution. The surface was previously formed in ATA and BTAH containing 3% NaCl solutions. The initial amount of adsorbed inhibitor was $51.1 \mu\text{g cm}^{-2}$ for ATA and $52.8 \mu\text{g cm}^{-2}$ for BTAH.

4. Conclusions

The current density of anodic and cathodic peaks in cyclic voltammograms decreased in the presence of inhibitors ATA and BTAH in 3% NaCl. The decrease of current density is a consequence of the formation of protective surface layer. The level of protection was dependent on the inhibitor concentration. BTAH provides better protection of copper at lower concentration than ATA. The exposure of copper in the presence of BTAH at concentration higher than 5 mM causes the formation of an amorphous precipitate, or precipitate with particles smaller than 10 nm. Species CuCl_2^- is assumed to be the major dissolved product in chloride medium.

EQCN corrosion and corrosion inhibition studies gave us valuable additional information on absolute mass change. Electrodeposition using potential control produced Cu-layer with smaller number of defects. Almost the same mass of inhibitor ATA and BTAH was adsorbed on copper surface after a one-hour immersion period. However, the film formed in the presence of BTAH showed much better inhibiting properties than the film formed in the presence of ATA.

5. Acknowledgements

The authors thank dr. Srečo Škapin of the Jožef Stefan Institute for X-ray diffraction measurements.

6. References

1. M. Fleischman, I. R. Hill, G. Mongoli, M. M. Musiani, *Electrochim. Acta*, **1983**, 28, 1325–1333.
2. D. Kuron, H. J. Rother, R. Holm, S. Storp, *Werkstoffe und Korrosion*, **1986**, 37, 83–93.
3. M. Beier, J. W. Schultze, *Electrochim. Acta*, **1992**, 37, 2299–2307.
4. J. B. Cotton, Proceedings of the Second International Congress on Metallic Corrosion, N.A.C.E, New York, **1963**.
5. M. Metikoš-Huković, R. Babić, A. Marinović, J. *Electrochem. Soc.*, **1998**, 145, 4045–4051.
6. R. Babić, M. Metikoš-Huković, M. Lončar, *Electrochim. Acta*, **1999**, 44, 2413–2421.
7. R. Youda, H. Nishihara, K. Aramaki, *Electrochim. Acta*, **1990**, 35, 1011–1017.
8. J. Wang: Analytical Electrochemistry, Second Edition, *John Wiley & Sons*, New York, 2000.
9. H. Otmačić, J. Telegdi, K. Papp, E. Stupnišek-Lisac, *J. Appl. Electrochem.*, **34** (2004) 545–550.
10. D. Tromans, R. Sun, *J. Electrochem. Soc.*, **1991**, 138, 3235–3244.
11. H. P. Lee, K. Nobe, *J. Electrochem. Soc.*, **1986**, 133, 2035–2043.
12. J. Crousier, L. Pardessus, J. P. Crousier, *Electrochim. Acta*, **1988**, 33, 1039–1042.
13. A. Kocijan, Ph. D. thesis, University of Ljubljana, Slovenia, 2004.
14. J. B. Cotton, I. R. Scoles, *Brit. Corros. J.*, **1967**, 2, 1–5.

Povzetek

Študirali smo inhibicijo korozije bakra v 3-odstotni raztopini natrijevega klorida z dodatkom različnih koncentracij organskega inhibitorja (3-amino-1,2,4-triazola – ATA in benzotriazola – BTAH). Eksperimente smo izvedli z različnimi elektrokemijskimi tehnikami: ciklično voltometrijo, linearno polarizacijo, Taflovimi in potenciodinamskimi krivuljami. Eksperimentalni rezultati so pokazali, da je BTAH učinkovitejši inhibitor kot ATA.

V tem delu smo uporabili tudi tehniko elektrokemijske kvarčne nanotehtnice (EQCN, *angl.* Electrochemical quartz crystal nanobalance) za raziskave depozicije bakra na zlato elektrodo pri kontroliranem potencialu ali pri kontroliranem toku. Rezultati so pokazali, da je nanos bakra primernejši pri metodi s kontroliranim potencialom. Študirali smo tudi tvorbo površinskih plasti po depoziciji bakra na zlato elektrodo v 3-odstotni raztopini natrijevega klorida v prisotnosti ATA ali BTAH. Izbrana korozijska inhibitorja sta pokazala zelo hitro interakcijo med kovino in organsko molekulo. Iz dobljenih rezultatov je jasno, da je tehnika EQCN zelo primerna pri pridobivanju *in-situ* informacij o inhibiciji korozije in njenem mehanizmu.